

Synthesis, Structure, and Coordination Chemistry of Aminophosphanlyboranes

Danan Dou,[†] Gerald W. Linti,[‡] Tuqiang Chen,[†] Eileen N. Duesler,[†] Robert T. Paine,^{*,†} and Heinrich Nöth^{*,‡}

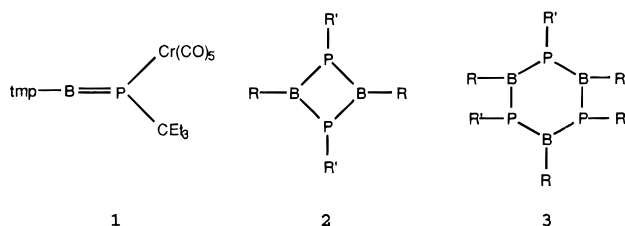
Department of Chemistry, University of New Mexico, Albuquerque, New Mexico 87131, and Institut für Anorganische Chemie, Universität München, 80333 München, Germany

Received November 9, 1995[⊗]

Syntheses for the diphosphadiboretane (${}^i\text{Pr}_2\text{NBPH}$)₂, the triphosphatriborinane (${}^i\text{Pr}_2\text{NBPH}$)₃, and the aminodiphosphanlyborane ${}^i\text{Pr}_2\text{NB}(\text{PH}_2)_2$ are reported. Reaction of these ligands with $\text{Cr}(\text{CO})_5\cdot\text{NMe}_3$ results in the formation of the complexes (${}^i\text{Pr}_2\text{NBPH}$)₂· $\text{Cr}(\text{CO})_5$ and ${}^i\text{Pr}_2\text{NB}(\text{PH}_2)_2\cdot 2\text{Cr}(\text{CO})_5$. Molecular structure determinations for the diphosphadiboretane, the triphosphatriborinane, and the two coordination complexes have been completed by use of single crystal X-ray diffraction techniques: (${}^i\text{Pr}_2\text{NBPH}$)₂ (C₆H₁₅BNP) crystallizes in the monoclinic space group $P2_1/n$ with $a = 7.7200(10)$ Å, $b = 10.514(2)$ Å, $c = 11.231(2)$ Å, $\beta = 101.100(10)^\circ$, and $Z = 4$; (${}^i\text{Pr}_2\text{NBPH}$)₃ (C₁₈H₄₅B₃N₃P₃) crystallizes in the monoclinic space group $P2_1/n$ with $a = 20.217(16)$ Å, $b = 13.764(11)$ Å, $c = 20.494(16)$ Å, $\beta = 104.40(5)^\circ$, and $Z = 8$; (${}^i\text{Pr}_2\text{NBPH}$)₂· $\text{Cr}(\text{CO})_5$ (C₁₇H₃₀B₂N₂O₅P₂Cr) crystallizes in the monoclinic space group $P2_1/n$ with $a = 11.284(3)$ Å, $b = 14.583(6)$ Å, $c = 16.515(4)$ Å, $\beta = 105.97(2)^\circ$, and $Z = 4$; ${}^i\text{Pr}_2\text{NB}(\text{PH}_2)_2\cdot[\text{Cr}(\text{CO})_5]_2$ (C₁₆H₁₈BNO₁₀P₂Cr₂) crystallizes in the orthorhombic space group $Fdd2$ with $a = 23.214(8)$ Å, $b = 11.914(5)$ Å, $c = 18.359(5)$ Å, and $Z = 8$.

Introduction

It has been previously observed that coordinatively unsaturated phosphanyl boranes, $\text{R}_2\text{B}-\text{PR}'_2$, are obtained as monomeric species when sterically demanding organic substituents are bonded to the electron deficient, three-coordinate boron atom.^{1–3} Without steric protection, however, these species typically self-associate, forming dimeric ($\text{R}_2\text{B}-\text{PR}'_2$)₂ and trimeric ($\text{R}_2\text{B}-\text{PR}'_2$)₃ ring compounds or oligomers with four-coordinate boron and phosphorus atom environments.^{1–5} Similarly, the more highly coordinatively unsaturated boranylidenephosphanes, $\text{RB}=\text{PR}'$, would also be expected to display a strong tendency to self-associate.³ Indeed, no monomeric examples have yet been isolated, although a $\text{Cr}(\text{CO})_5$ adduct **1** of $\text{tmpB}=\text{PCEt}_3$ ($\text{tmp} = 2,2,6,6\text{-tetramethylpiperidino}$) has been characterized.⁶ All other efforts to obtain the elusive boranylidenephosphanes have resulted instead in the formation of four-membered ($\text{RB}-\text{PR}'$)₂ **2** or six-membered ($\text{RB}-\text{PR}'$)₃ **3** ring compounds containing three-coordinate boron and phosphorus atoms.^{1–3} The ring size adopted appears to depend on the size of the substituent groups R and R'. For example, Power and co-workers^{1,2,7,8} noted that, with less bulky aryl and alkyl group combinations ($\text{R/R}' = \text{Mes/Cy}$, Mes/Ph , Mes/Mes , and Ph/Mes), *planar* six-membered rings formed, while slightly larger organic group combinations ($\text{R/R}' = \text{Mes}/1\text{-Ad}$ and Thex/Mes) produced



planar four-membered rings. A mixture of four- and six-membered rings was obtained with $\text{R/R}' = \text{Mes}/t\text{-Bu}$. Recently, similar behavior was found with compounds containing amino substituents on the boron atoms,⁹ larger amino groups ($\text{R/R}' = \text{Ph}_2\text{N/H}$ and tmp/H) gave *planar* four-membered rings, while smaller amino groups ($\text{R/R}' = \text{Me}_2\text{N/H}$ and $\text{Et}_2\text{N/H}$) resulted in *nonplanar*, twisted six-membered ring geometries. The only exception so far to this steric trend was found with the bulky but more weakly π donating amido group $(\text{Me}_3\text{Si})_2\text{N}$, which produced a *nonplanar* six-membered ring structure.⁹

During our earlier investigations, it was observed that the outcome of reactions of ${}^i\text{Pr}_2\text{NBCL}_2$ with $\text{LiPH}_2\cdot\text{DME}$ was sensitive to reagent stoichiometry and reaction conditions.⁹ The evidence available at that time suggested that perhaps both four-membered ($n = 2$) and six-membered ($n = 3$) ring compounds (${}^i\text{Pr}_2\text{NBPH}$)_n were produced, but their separation and isolation were not successfully completed. We have continued to examine this system since the rings offer potentially useful building blocks for the synthesis of polycyclic cage compounds. We report here on approaches that allow for the synthesis of pure samples of (${}^i\text{Pr}_2\text{NBPH}$)₂ and (${}^i\text{Pr}_2\text{NBPH}$)₃. In addition, we describe the molecular structure determinations of both ring compounds and the formation of metal coordination complexes of (${}^i\text{Pr}_2\text{NBPH}$)₂ and the reactive intermediate ${}^i\text{Pr}_2\text{NB}(\text{PH}_2)_2$.

Experimental Section

General Information. Standard inert atmosphere techniques were used for the manipulation of all reagents and reaction products. Infrared spectra were recorded on a Matteson 2020 FT-IR spectrometer from

[†] University of New Mexico.

[‡] Universität München.

[⊗] Abstract published in *Advance ACS Abstracts*, May 1, 1996.

- Power, P. P. *Angew. Chem., Intl. Ed. Engl.* **1990**, *29*, 449 and references therein.
- Power, P. P.; Moezzi, A.; Pestana, D. C.; Petrie, M. A.; Shoner, S. C.; Waggoner, K. M. *Pure Appl. Chem.* **1991**, *63*, 859.
- Paine, R. T.; Nöth, H. *Chem. Rev.* **1995**, *95*, 343.
- Sowerby, D. B. *The Chemistry of Inorganic Homo- and Heterocycles*; Haiduc, I., Sowerby, D. B., Eds.; Academic Press: New York, 1987; Vol. I, Chapter 3.
- Nöth, H.; Staude, S.; Thomann, M.; Paine, R. T. *Chem. Ber.* **1993**, *126*, 611.
- Linti, G.; Nöth, H.; Polborn, K.; Paine, R. T. *Angew. Chem., Intl. Ed. Engl.* **1990**, *29*, 682.
- Rasika Dias, H. V.; Power, P. P. *Angew. Chem., Intl. Ed. Engl.* **1987**, *26*, 1270.
- Rasika Dias, H. V.; Power, P. P. *J. Am. Chem. Soc.* **1989**, *111*, 144.

(9) Dou, D.; Westerhausen, M.; Wood, G. L.; Duesler, E. N.; Nöth, H.; Paine, R. T. *Chem. Ber.* **1993**, *126*, 379.

Table 1. Crystallographic Data for $(\text{Pr}_2\text{NBPH})_2$ (**4**), $(\text{Pr}_2\text{NBPH})_3$ (**5**), $(\text{Pr}_2\text{NBPH})_2\cdot\text{Cr}(\text{CO})_5$ (**6**), and $\text{Pr}_2\text{NB}[(\text{PH}_2)\cdot\text{Cr}(\text{CO})_5]_2$ (**7**)

	4	5	6	7
chem formula	$\text{C}_6\text{H}_{15}\text{BNP}$	$\text{C}_{18}\text{H}_{45}\text{B}_3\text{N}_3\text{P}_3$	$\text{C}_{17}\text{H}_{30}\text{B}_2\text{N}_2\text{O}_5\text{P}_2\text{Cr}$	$\text{C}_{16}\text{H}_{18}\text{BNO}_{10}\text{P}_2\text{Cr}_2$
<i>a</i> , Å	7.720(1)	20.217(16)	11.284(3)	23.214(8)
<i>b</i> , Å	10.514(2)	13.764(11)	14.583(6)	11.914(5)
<i>c</i> , Å	11.231(2)	20.494(16)	16.515(4)	18.359(5)
α , deg	90	90	90	90
β , deg	101.10(1)	104.40(5)	105.97(2)	90
γ , deg	90	90	90	90
<i>V</i> , Å ³	894.5(3)	5524(8)	2613(1)	5077(3)
<i>Z</i>	4	8	4	8
ρ_{calcd} , g cm ⁻³	1.062	1.032	1.215	1.468
fw	143.0	428.9	478.0	561.1
cryst system	monoclinic	monoclinic	monoclinic	orthorhombic
space group	<i>P2</i> ₁ / <i>n</i>	<i>P2</i> ₁ / <i>n</i>	<i>P2</i> ₁ / <i>n</i>	<i>Fdd2</i>
<i>T</i> , °C	20	20	20	20
μ , mm ⁻¹	0.225	0.218	0.572	1.004
λ (Mo K α), Å	0.71073	0.71073	0.71073	0.71073
<i>R</i> _F ^a	0.047	0.059	0.0997	0.096
<i>R</i> _{wF} ^b	0.043	0.076	0.047	0.087

$$^a R_F = \sum ||F_o| - |F_c|| / \sum |F_o|. \quad ^b R_{wF} = [\sum w(|F_o| - |F_c|)^2 / \sum w F_o^2]^{1/2}.$$

KBr pellets, and mass spectra were recorded on a Finnegan GC/MS using a solids inlet probe and on a Kratos MS-50 spectrometer with FAB analysis. NMR spectra were recorded on Bruker WP-250 and JEOL GSX-400 spectrometers. All NMR spectra were referenced with Me₄Si (¹³C and ¹H), BF₃·OEt₂ (¹¹B), and 85% H₃PO₄ (³¹P) with + δ = downfield. The samples were contained in sealed 5 mm tubes and dissolved in a deuterated lock solvent. Elemental analyses were from the UNM analytical services laboratory.

Materials. Reagents Pr_2NBCl_2 ,¹⁰ $\text{LiPH}_2\cdot\text{DME}$,¹¹ $[\text{Pr}_2\text{NB}(\text{H})(\text{Pr}_2\text{N})\text{BPLi}\cdot\text{DME}]$,^{9,12} and $\text{Cr}(\text{CO})_5\cdot\text{NMe}_3$ ¹³ were prepared by literature methods. The BuLi and ^tBuLi solutions (Aldrich) were used as received. Solvents were dried and degassed by standard methods, and solvent transfers were accomplished by vacuum distillation.

Synthesis and Characterization of Compounds. 2,4-Bis(diisopropylamino)-1,3,2,4-diphosphadiboretane (4). A solution containing $[\text{Pr}_2\text{NBP}(\text{H})(\text{Pr}_2\text{N})\text{BPLi}\cdot\text{DME}]$ (1.58 g, 4.15 mmol) in Et₂O (30 mL) was cooled to 0 °C, and a solution of anhydrous HCl (4.15 mmol) in Et₂O (20 mL) was added dropwise very slowly over ~2 h (~4 drops min⁻¹). Slow addition is required to avoid undesired side reactions. A white precipitate (LiCl) forms immediately upon addition of the HCl/Et₂O solution and continues to form during the reaction. After the addition was complete, the reaction mixture was warmed to 23 °C and stirred (3 h). The solvent was vacuum evaporated and the residue extracted with hexane (20 mL). The mixture was filtered and the filtrate concentrated to 10 mL. This solution was cooled (-10 °C), and colorless single crystals of **4** formed: yield 0.52 g (44%); mp 127–129 °C. Mass spectrum (30 eV) *m/e*: 286 (95, M⁺), 253 (100), 173 (23), 158 (20), 110 (41). Infrared spectrum (hexane, cm⁻¹): 2268 (PH, w), 1479 (w), 1441 (w), 1398 (w), 1368 (s), 1312 (s), 1248 (w), 1186 (s), 1148 (s), 1115 (w), 1007 (w), 872 (w), 839 (m), 808 (m), 791 (m), 777 (m), 758 (w), 673 (w), 575 (w), 505 (w), 494 (w). Anal. Calcd for C₁₂H₃₀B₂N₂P₂ (285.95): C, 50.40; H, 10.57; N, 9.80. Found: C, 50.74; H, 11.12; N, 9.68.

2,4,6-Tris(diisopropylamino)-1,3,5,2,4,6-triphosphatriborinane (5). A suspension of $\text{LiPH}_2\cdot\text{DME}$ (0.75 g, 5.8 mmol) in Et₂O (25 mL) was added slowly with stirring to a solution of Pr_2NBCl_2 (0.52 g, 2.9 mmol) in pentane (25 mL) at 23 °C. The PH₃ produced in the reaction was continuously released through a mercury bubbler. After 5 h, the solvents were removed by vacuum evaporation and additional pentane (10 mL) was condensed onto the residue. The insoluble fraction (LiCl) was removed by filtration, and the filtrate was vacuum evaporated. A pale yellow oil remained that slowly crystallized over several days at

23 °C: yield 0.39 g (95%); mp 100–102 °C (dec). Mass spectrum (HRMS-FAB, 70 eV) *m/e*: 429.3095 (M⁺, ¹²C₁₈H₄₅¹⁴N₃³¹P₃B₃, 429.3111, dev 1.2 ppm), 395 (100), 366 (11), 286 (21), 253 (41), 198 (10), 110 (38). Anal. Calcd for C₁₈H₄₅N₃B₃P₃ (429.31): C, 50.40; H, 10.58; N, 9.80. Found: C, 51.26; H, 10.47; N, 9.82.

[2,4-Bis(diisopropylamino)-1,3,2,4-diphosphadiboretane]chromium Pentacarbonyl (6). A sample of Pr_2NBCl_2 (1.4 g, 7.7 mmol) dissolved in hexane (50 mL) was combined with $\text{LiPH}_2\cdot\text{DME}$ (1.9 g, 14.6 mmol) at -78 °C. The mixture was stirred (2 h), warmed to 23 °C, and stirred (16 h). The white cloudy solution was filtered and the solvent removed from the filtrate by vacuum evaporation. The residue containing **4** was redissolved in hexane (50 mL), and $\text{Cr}(\text{CO})_5\cdot\text{NMe}_3$ (1.93 g, 7.7 mmol) was added to the solution at 23 °C. This mixture was stirred (16 h), whereupon the solvent was removed by vacuum evaporation until ~5 mL of solution remained. This solution was cooled (-10 °C), and yellow single crystals of **6** deposited: yield 0.5 g (14%); mp 170–172 °C (dec). Mass spectrum (30 eV) *m/e*: 422 (1, M⁺-2CO), 394 (2), 366 (23), 338 (100), 225 (40) 195 (12), 163 (18), 151 (20). Infrared spectrum (hexane, cm⁻¹): 2315 (w), 2276 (w), 2056 (m), 1956 (s), 1935 (vs), 1908 (m), 1483 (w), 1368 (w), 1323 (w), 1184 (w), 1150 (w), 725 (w), 671 (w), 656 (w), 461 (w). Anal. Calcd for C₁₇H₃₀B₂N₂O₅P₂Cr (478.001): C, 42.72; H, 6.33; N, 5.86. Found: C, 42.62; H, 6.42; N, 5.90.

[(Diisopropylamino)bis(phosphanylborane)]bis(chromium Pentacarbonyl) (7). A sample of Pr_2NBCl_2 (1.45 g, 7.97 mmol) was dissolved in hexane (25 mL), and $\text{LiPH}_2\cdot\text{DME}$ (1.97 g, 15.1 mmol) was added to the solution at -78 °C. The mixture was stirred briefly at -78 °C and then warmed to 23 °C and stirred (16 h). The white cloudy mixture was filtered and the filtrate evaporated to dryness. The residue was redissolved in hexane (5 mL), and 4.0 g (16 mmol) of $\text{Cr}(\text{CO})_5\cdot\text{NMe}_3$ in hexane (10 mL) added. This mixture was stirred at 23 °C (16 h) and the resulting solution evaporated to dryness. The residue was recrystallized from cold hexane (5 mL), and yellow single crystals of **7** deposited: yield 1.5 g (34%); mp 105–107 °C. Mass spectrum (30 eV) *m/e*: 561 (M⁺, 30), 449 (12), 421 (42), 393 (40), 281 (25), 257 (18), 229 (15), 113 (20). Infrared spectrum (hexane, cm⁻¹): 2349 (w), 2065 (s), 1985 (s), 1948 (vs), 1485 (w), 1370 (w), 1337 (w), 1213 (w), 1194 (w), 1138 (w), 1020 (m), 785 (w), 671 (s), 658 (s). Anal. Calcd for C₁₆H₁₈BNO₁₀P₂Cr₂ (561.07): C, 34.25; H, 3.23; N, 2.50. Found: C, 34.22; H, 3.13; N, 2.60.

Crystallographic Measurements and Structure Solution. Crystals of **4** (0.23 × 0.30 × 0.37 mm), **5** (0.40 × 0.35 × 0.55 mm), **6** (0.12 × 0.16 × 0.53 mm), and **7** (0.21 × 0.30 × 0.35 mm) were placed in glass capillaries under dry nitrogen. The crystals were centered on a Syntex P3/F automated diffractometer, and determinations of crystal class, orientation matrix, and unit cell dimensions were performed in a standard manner. A summary of crystallographic data is given in Table 1. Data (**4**, $\pm h, k, \pm l$; **5**, $+h, +k, \pm l$; **6**, $\pm h, \pm k, -l$; **7**, $\pm h, \pm k, \pm l$) were collected in the ω scan mode with Mo K α ($\lambda = 0.71073$ Å) radiation, a scintillation counter, and a pulse height analyzer. In each

- (10) Gerrard, W.; Hudson, H. R.; Mooney, E. R. *J. Chem. Soc.* **1960**, 5168.
 (11) Schäfer, H.; Fritz, G.; Hölderich, W. *Z. Anorg. Allg. Chem.* **1977**, 428, 222.
 (12) Dou, D.; Kaufmann, B.; Duesler, E. N.; Chen, T.; Paine, R. T.; Nöth, H. *Inorg. Chem.* **1993**, 32, 3056.
 (13) Wasserman, H. J.; Workulich, M.; Atwood, J. D.; Churchill, M. R. *Inorg. Chem.* **1980**, 19, 2831.

Table 2. Atomic Coordinates ($\times 10^4$) and Their Esd's for $(i\text{Pr}_2\text{NBPH})_2$ (**4**)

	<i>x</i>	<i>y</i>	<i>z</i>	<i>U</i> (eq) ^a
P	1678(1)	5180(1)	9661(1)	58(1)
B	626(3)	4032(3)	10660(2)	38(1)
N	1353(2)	3010(2)	11344(2)	40(1)
C(1)	3239(3)	2678(2)	11408(2)	48(1)
C(2)	3474(4)	1325(3)	11005(3)	71(1)
C(3)	4319(3)	2946(3)	12671(3)	74(1)
C(4)	386(3)	2192(2)	12075(2)	45(1)
C(5)	-1112(4)	1483(3)	11265(3)	65(1)
C(6)	-242(4)	2921(3)	13072(2)	61(1)

^a Equivalent isotropic *U* defined as one-third of the trace of the orthogonalized U_{ij} tensor.

case, inspection of a small data set led to assignment of the indicated space groups.¹⁴ Empirical absorption corrections were applied to the data, on the basis of ψ scans¹⁵ ($T_{\text{min,max}}$, **4**, 0.93, 0.955; **6**, 0.89, 0.93; **7**, 0.69, 0.80). Some signs of crystal decay were noted for **7**.

All calculations were performed with a Siemens SHELXTL PLUS (Microvax II version) structure determination system.¹⁶ Solutions for the data sets were by direct methods, and full matrix refinements were employed.¹⁷ Neutral atom scattering factors and anomalous dispersion terms were used for all non-hydrogen atoms during the refinements. The function minimized was $\sum w(|F_o| - |F_c|)^2$. All non-hydrogen atoms in **4** were refined anisotropically, and the final *R* values were $R_F = 0.047$ and $R_{wF} = 0.043$ on 1163 observed reflections ($F > 3\sigma(F)$). The methyl hydrogen atoms were placed in idealized positions with $U_{\text{iso}} = 1.25U_{\text{eq}}$ (riding model). The resulting difference map showed the phosphorus H atoms in two positions. These positions were allowed to vary with $U_{\text{iso}} = 1.25U_{\text{eq}}$ of the P atom, and the final occupancies for H(1a) and H(1b) were 0.58(3) and 0.42(3), respectively. The slight difference may be due to the fact that H(1b) is closer to another H atom than is H(1a): H(6b)⋯H(1b) ($-x, 1-y, 2-z$) = 2.474 Å and H(5c)⋯H(1a) ($-x, 1-y, 2-z$) = 2.591 Å. The refinement for **5** was straightforward giving final *R* values of $R_F = 0.059$ and $R_{wF} = 0.076$ on 3632 reflections ($R > 4\sigma(F)$). The refinement for **6** was treated in a similar fashion and the final *R* values were $R_F = 0.0997$ and $R_{wF} = 0.047$ on 2130 reflections ($F > 2\sigma(F)$). Refinement of **7** gave the final *R* values of $R_F = 0.096$ and $R_{wF} = 0.087$ on 1238 reflections ($F > 2\sigma(F)$), and it was revealed that C(8) was disordered over two sites with occupancies of 54%, C(8), and 46%, C(8''). All H atoms except H(1a) on P were placed in idealized positions with $U_{\text{iso}} = 1.25U_{\text{eq}}$ (riding model). H(1a) was fixed in the position found in the difference map but adjusted so that the P-H bond distance was 1.2 Å. The polarity of the crystal was tested by inverting the molecule and refining. This showed that all oxygen and carbon atoms (except C(8); C(8'')) became nonpositive-definite, and $R = 33\%$. Refinement with all atoms isotropic (68 parameters) gave $R = 35\%$ with bond distances and angles deviating substantially from expected values. Listings of the non-hydrogen atom coordinates are given in Tables 2-5. Additional crystallographic parameters and details of the structure solutions (Table S-1), hydrogen atom positional parameters (Table S-5), full listings of bond distances and angles (Tables S-2 and S-3), and anisotropic thermal parameters (Table S-4) are provided in Supporting Information.

(14) Space group notation is given in *International Tables for X-Ray Crystallography*; Reidel: Dordrecht, Holland, 1983; Vol. I, pp 73-346.

(15) The empirical absorption corrections use an ellipsoidal model fitted to azimuthal scan data that are then applied to the intensity data: *SHELXTL Manual, Revision 4*; Nicolet XRD Corp.: Madison, WI, 1983.

(16) Sheldrick, G. M. *Nicolet SHELXTL Operations Manual*; Nicolet XRD Corp.: Cupertino, CA, 1981. SHELXTL uses absorption, anomalous dispersion, and scattering data compiled in *International Tables for X-Ray Crystallography*; Kynoch: Birmingham, England, 1974; Vol. IV, pp 55-60, 99-101, 149-150. Anomalous dispersion terms were included for all atoms with atomic numbers greater than 2.

(17) A general description of the least-squares algebra is found in *Crystallographic Computing*; Ahmed, F. R., Hall, S. R., Huber, C. P., Eds.; Munksgaard: Copenhagen, 1970; p 187. The least-squares refinement minimizes $\sum w(|F_o - F_c|)^2$, where $w = 1/[\sigma(F)^2 + gF^2]$.

Table 3. Atomic Coordinates ($\times 10^4$) and Their Esd's for $(i\text{Pr}_2\text{NBPH})_3$ (**5**)

	<i>x</i>	<i>y</i>	<i>z</i>	<i>U</i> (eq)
P(1)	4479(1)	2176(1)	7413(1)	77(1)
P(2)	3029(1)	1011(1)	7059(1)	81(1)
P(3)	2995(1)	3224(2)	7189(1)	81(1)
B(1)	4000(3)	1006(5)	7501(3)	59(3)
B(2)	2916(3)	2192(5)	6532(4)	62(3)
B(3)	3983(4)	3331(5)	7520(3)	59(3)
N(1)	4302(3)	129(3)	7762(2)	63(2)
C(1)	5041(3)	-66(5)	8032(3)	75(3)
C(2)	5458(3)	158(5)	7523(4)	108(4)
C(3)	5336(3)	401(6)	8705(4)	114(4)
C(4)	3889(3)	-768(4)	7729(3)	72(3)
C(5)	3989(3)	-1288(5)	8400(3)	101(4)
C(6)	3993(4)	-1463(5)	7185(4)	115(4)
N(2)	4276(3)	4225(3)	7743(2)	62(2)
C(7)	2695(4)	1489(6)	5346(4)	95(4)
C(8)	2106(5)	858(6)	5260(4)	143(5)
C(9)	3359(4)	1003(6)	5371(4)	132(5)
C(10)	2606(5)	3261(6)	5487(4)	114(4)
C(11)	3226(6)	3604(7)	5281(5)	177(7)
C(12)	1933(5)	3387(7)	5029(5)	165(6)
N(3)	2734(2)	2290(4)	5836(3)	68(2)
C(13)	3841(3)	5084(4)	7775(3)	71(3)
C(14)	3787(4)	5758(5)	7178(3)	115(4)
C(15)	4047(4)	5654(5)	8431(3)	99(4)
C(16)	5019(4)	4457(5)	7894(4)	83(3)
C(17)	5435(3)	4053(5)	8554(4)	100(4)
C(18)	5328(4)	4288(6)	7310(4)	121(4)
P(1')	2381(1)	6467(1)	4276(1)	75(1)
P(2')	1125(1)	7593(2)	3422(1)	84(1)
P(3')	2578(1)	8641(1)	3740(1)	80(1)
B(1')	1582(3)	7199(5)	4326(4)	59(3)
B(2')	1894(4)	7991(5)	3051(4)	66(3)
B(3')	3002(4)	7530(5)	4238(3)	61(3)
N(1')	1304(3)	7344(3)	4881(3)	64(2)
C(1')	1641(4)	7134(6)	5592(4)	92(4)
C(2')	1680(4)	6072(6)	5765(4)	126(5)
C(3')	2289(4)	7694(6)	5846(4)	88(3)
C(4')	613(4)	7819(5)	4789(4)	88(3)
C(5')	112(4)	7241(6)	5051(4)	123(4)
C(6')	692(4)	8859(6)	5019(4)	130(5)
N(2')	1866(3)	7862(4)	2372(3)	71(2)
C(7')	1269(4)	7359(6)	1910(4)	95(4)
C(8')	829(4)	8066(7)	1432(4)	153(5)
C(9')	1466(4)	6467(6)	1595(4)	126(5)
C(10')	2374(4)	8217(7)	2027(4)	107(4)
C(11')	2435(5)	9297(7)	2003(4)	154(5)
C(12')	3036(4)	7660(7)	2213(4)	136(5)
N(3')	3700(3)	7509(40)	4544(3)	79(3)
C(13')	4107(4)	6694(7)	4854(4)	113(4)
C(14')	4095(5)	5870(6)	4396(4)	142(5)
C(15')	4035(4)	6366(6)	5546(6)	120(4)
C(16')	4137(4)	8427(7)	4574(4)	119(4)
C(17')	4575(4)	8364(7)	4079(5)	141(5)
C(18')	4437(5)	8770(6)	5251(4)	

^a Equivalent isotropic *U* defined as one-third of the trace of the orthogonalized U_{ij} tensor.

Results and Discussion

We have previously reported⁹ that 1:2 reactions of tmpBCl₂ (tmp = 2,2,6,6-tetramethylpiperidino) and LiPH₂·DME in hexane or diethyl ether provide good yields (85-95%) of the cyclic diphosphadiboretane (tmpBPH)₂. The 1:2 reaction of ⁱPr₂NBCl₂ with LiPH₂·DME in hexane in a closed reaction flask, on the other hand, gave complex product mixtures that contained an unidentified compound (~80%, ³¹P NMR δ -151, $J_{\text{PH}} = 188$ Hz), [ⁱPr₂NBP(H)(ⁱPr₂N)BPLi·DME] (**9**) (~15%, ³¹P NMR δ -174.9, -91.2, $J_{\text{PP}} = 52$ Hz, $J_{\text{PH}} = 146$ Hz), ⁱPr₂NB(PH₂)₂ (~1%, ³¹P NMR δ -191.7, $J_{\text{PH}} = 205$ Hz), and the novel cage species (ⁱPr₂NB)₃P₂¹⁸ (~1%, ³¹P NMR δ -13). An additional product, obtained in low yield, was attributed to (ⁱPr₂NBPH)₂

Table 4. Atomic Coordinates ($\times 10^4$) and Their Esd's for $(^i\text{Pr}_2\text{NBPH})_2\cdot\text{Cr}(\text{CO})_5$ (**6**)

	x	y	z	U(eq)
Cr	6222(1)	8074(1)	4166(1)	52(1)
C(1)	7213(9)	8100(1)	5244(6)	84(5)
O(1)	7820(6)	8133(7)	5940(4)	120(4)
C(2)	7554(8)	8417(6)	3733(6)	62(5)
O(2)	8359(6)	8618(5)	3483(5)	101(4)
C(3)	5804(8)	9319(7)	4182(6)	62(5)
O(3)	5580(7)	10083(5)	4206(4)	95(4)
C(4)	4889(8)	7750(6)	4591(5)	62(4)
O(4)	4114(6)	7559(5)	4871(4)	103(4)
C(5)	6591(9)	6830(7)	4078(6)	79(5)
O(5)	6805(9)	6070(5)	4004(6)	134(5)
P(1)	4901(2)	7978(2)	2746(1)	42(1)
P(2)	4865(2)	9438(2)	1615(2)	63(1)
B(1)	3777(9)	8962(7)	2235(6)	47(4)
B(2)	5506(8)	8202(7)	1748(6)	41(4)
N(1)	2664(6)	9210(4)	2342(4)	48(3)
N(2)	6168(6)	7663(4)	1373(4)	45(3)
C(6)	2132(8)	8703(6)	2938(6)	62(4)
C(7)	915(8)	8239(8)	2490(6)	114(6)
C(8)	2019(9)	9298(7)	3666(6)	114(6)
C(9)	1893(9)	9984(7)	1892(6)	74(5)
C(10)	2601(10)	10874(6)	2029(7)	117(7)
C(11)	1365(8)	9757(8)	964(6)	118(6)
C(12)	6555(8)	7946(7)	614(6)	67(5)
C(13)	5462(9)	8065(7)	-151(5)	103(6)
C(14)	7342(8)	8790(6)	792(6)	88(5)
C(15)	6539(9)	6734(6)	1682(6)	75(5)
C(16)	5972(9)	5994(6)	1050(7)	121(7)
C(17)	7925(9)	6626(6)	2004(6)	117(6)

^a Equivalent isotropic U defined as one-third of the trace of the orthogonalized U_{ij} tensor.

Table 5. Atomic Coordinates ($\times 10^4$) and Their Esd's for $^i\text{Pr}_2\text{NB}[(\text{PH}_2)_2\cdot\text{Cr}(\text{CO})_5]_2$ (**7**)

	x	y	z	U(eq)
Cr	3009(1)	36(2)	0	75(1)
P	2274(2)	1248(3)	454(3)	64(1)
B	2500	2500	1074(13)	45(7)
N	2500	2500	1820(10)	66(7)
O(1)	3929(7)	-1368(12)	-679(11)	143(9)
O(2)	2976(7)	-1533(12)	1302(13)	151(8)
O(3)	3905(5)	1419(9)	779(9)	109(6)
O(4)	2100(5)	-1410(10)	-729(9)	140(8)
O(5)	3059(7)	1503(13)	-1349(9)	127(8)
C(1)	3551(9)	-881(20)	-385(14)	115(11)
C(2)	2973(9)	-915(6)	803(14)	102(10)
C(3)	3585(7)	885(11)	511(11)	70(6)
C(4)	2444(6)	-858(13)	-444(11)	84(7)
C(5)	3059(7)	977(16)	-848(11)	73(7)
C(6)	2702(8)	3441(18)	2255(13)	124(10)
C(7)	3287(9)	3380(15)	2476(16)	162(13)
C(8)	2404(20)	4349(30)	2270(25)	88(8)
C(8'')	2184(23)	4210(35)	2581(34)	88(8)

^a Equivalent isotropic U defined as one-third of the trace of the orthogonalized U_{ij} tensor.

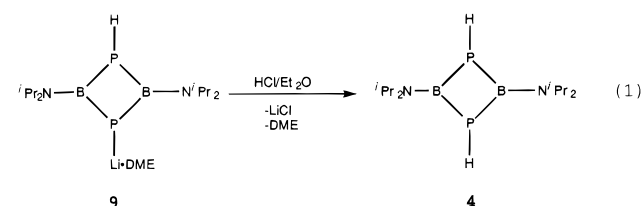
(**4**) (~1%, ^{31}P NMR δ -162.8, $J_{\text{PH}} = 111$ Hz). Furthermore, the relative yields of these products were found to change as a function of reaction conditions and reagent stoichiometry. Through careful control of reagent stoichiometry, it was found that **9** and $(^i\text{Pr}_2\text{NB})_3\text{P}_2$ ¹⁸ could be isolated with high yields and good purities. However, until now it has remained impossible to obtain pure samples of $^i\text{Pr}_2\text{NB}(\text{PH}_2)_2$ (**8**) or the two products characterized only by the ^{31}P NMR resonances at δ -151 (unidentified) and -162.8 (**4**).

Table 6. NMR Data for Phosphanylboranes (20 °C, C_6D_6)^a

compound	$\delta(^{31}\text{P})$	$\delta(^{11}\text{B})$	$\delta(^1\text{H})$	$\delta(^{13}\text{C})$
$(^i\text{Pr}_2\text{NBPH})_2$ (4)	-162.8	47.1	1.18 (CH ₃) 3.54 (CH) 3.43 (PH)	23.2 (CH ₃) 51.6 (CH)
$(^i\text{Pr}_2\text{NBPH})_3$ (5)	-151	49.8	1.21 (CH ₃) 3.98 (CH) 3.35 (PH)	22.8 (CH ₃) 51.2 (CH)
$(^i\text{Pr}_2\text{NBPH})_2\cdot\text{Cr}(\text{CO})_5$ (6)	-124.2 -148.4	44.2	0.88 (CH ₃) 1.09 (CH ₃) 1.11 (CH ₃) 3.67 (CH) 3.06 (CH) 3.65 (PH)	24.1 (CH ₃) 21.7 (CH ₃) 56.7 (CH) 47.6 (CH)
$^i\text{Pr}_2\text{NB}(\text{PH}_2)_2$ (8)	-191.7	48.9		
$^i\text{Pr}_2\text{NB}[(\text{PH}_2)_2\cdot\text{Cr}(\text{CO})_5]_2$ (7)	-127.9	41.4	0.85 (CH ₃) 3.1 (CH) 3.0 (PH)	23.0 (CH ₃) 53.9 (CH) 216.7 (CO) 220.8 (CO)

^a Coupling constants (Hz): **4**, $^1J_{\text{PH}} = 244.3$, $^3J_{\text{PC}} = 5.0$, $^3J_{\text{HH}} = 6.8$, $^3J_{\text{HH}} = 6.8$; **5**, $^1J_{\text{PH}} = 238$, $^3J_{\text{PH}} = 15$, $^3J_{\text{HH}} = 7$; **6**, $^1J_{\text{PH}} = 200$, $^1J_{\text{PP}} = 177.5$, $^4J_{\text{PC}} = 15.5$, $^3J_{\text{PC}} = 10.6$, $^3J_{\text{PC}} = 4.7$, $^3J_{\text{PC}} = 6.9$, $^2J_{\text{PC}} = 9.7$, $^2J_{\text{PC}} = 6.3$, $^3J_{\text{HH}} = 6.7$, $^3J_{\text{HH}} = 6.5$; **7**, $^1J_{\text{PH}} = 310$, $^2J_{\text{PC}} = 5.4$, $^2J_{\text{PC}} = 3.2$, $^3J_{\text{HH}} = 6.8$ Hz.

Since large samples of pure $[^i\text{Pr}_2\text{NBP}(\text{H})(^i\text{Pr}_2\text{N})\text{BPLi}\cdot\text{DME}]$ (**9**) are available from the 1:2.5 ratio reaction of $^i\text{Pr}_2\text{NBCl}_2$ and $\text{LiPH}_2\cdot\text{DME}$,¹² a convenient synthesis for **4** should arise from careful protonation of this salt. Combination of **9** with anhydrous HCl diluted in Et_2O at 0 °C in a 1:1 ratio produces $(^i\text{Pr}_2\text{NBPH})_2$ (**4**) exclusively (eq 1). However, the rate of



addition of the HCl/ Et_2O solution to the solution of **9** is crucial. If the addition of acid is too fast, a competitive parasitic reaction of HCl with the B-P bonds occurs with subsequent ring cleavage and formation of $^i\text{Pr}_2\text{NBCl}_2$. When the reaction is properly performed, NMR analysis of the resulting reaction mixture shows greater than 90% conversion of **9** to **4**. Reasonably pure powdered samples of colorless **4** are obtained by solvent evaporation followed by recrystallization from hexane. The high solubility of **4** in hexane, however, makes high-yield recovery following repeated recrystallizations impossible. Typically, analytically pure crystalline samples of **4** are isolated in 40–50% overall yield following two recrystallizations, although additional material can be harvested from collected mother liquors.

Compound **4** displays a strong parent ion ($m/e = 286$) in the EI-MS spectrum that confirms the composition. The molecule would be expected to display both symmetric and asymmetric P-H stretching frequencies, but only a single P-H infrared frequency at 2268 cm^{-1} is resolved. The latter is comparable with the ν_{PH} values observed for $(\text{tmpBPH})_2$ and $[(\text{Me}_3\text{Si})_2\text{NBPH}]_3$.⁹ The ^1H , ^{13}C , ^{11}B , and ^{31}P NMR spectra for **4** are summarized in Table 6. It is most important to note that **4** displays a single resonance δ -162.8 in the $^{31}\text{P}\{^1\text{H}\}$ NMR spectrum that provides an unambiguous signature for this compound in reaction mixtures obtained from previously reported combinations of $^i\text{Pr}_2\text{NBCl}_2$ with $\text{LiPH}_2\cdot\text{DME}$.⁹ The resonance splits into a "pseudotriplet" pattern resulting from

(18) Dou, D.; Wood, G. L.; Duesler, E. N.; Paine, R. T.; Nöth, H *Inorg. Chem.* **1992**, *31*, 3756.

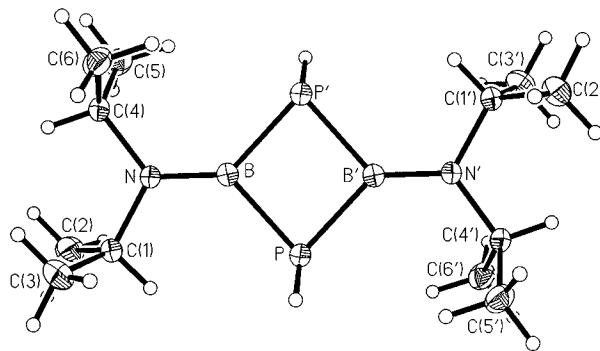
Table 7. Selected Bond Lengths (Å) and Bond Angles (deg) for (ⁱPr₂NBPH)₂ (**4**), (ⁱPr₂NBPH)₃ (**5**), (ⁱPr₂NBPH)₂·Cr(CO)₅ (**6**), and ⁱPr₂NB[PH₂·Cr(CO)₅]₂ (**7**)

4		5				6		7	
		molecule 1		molecule 2					
Bond Lengths									
P–B	1.930(3)	P(1)–B(1)	1.911(7)	P(1')–B(1')	1.929(7)	P(1)–B(1)	1.947(9)	P–B	1.95(1)
P–B'	1.932(3)	P(1)–B(3)	1.922(8)	P(1')–B(3')	1.942(8)	P(1)–B(2)	1.977(10)	P'–B	1.95(1)
		P(2)–B(2)	1.933(8)	P(2')–B(2')	1.972(9)	P(2)–B(1)	1.931(11)		
		P(2)–B(1)	1.947(7)	P(2')–B(1')	1.931(7)	P(2)–B(2)	1.933(10)		
		P(3)–B(2)	1.938(8)	P(3')–B(2')	1.931(7)				
		P(3)–B(3)	1.947(7)	P(3')–B(3')	1.920(7)				
B–N	1.377(3)	B(1)–N(1)	1.399(8)	B(1')–N(1')	1.403(10)	B(1)–N(1)	1.365(13)	B–N	1.37(3)
		B(2)–N(3)	1.387(10)	B(2')–N(2')	1.390(10)	B(2)–N(2)	1.346(12)		
		B(3)–N(2)	1.392(8)	B(3')–N(3')	1.395(9)				
						Cr–P(1)	2.412(2)	Cr–P	2.385(5)
						Cr–CO _{trans}	1.824(9)	Cr–CO _{trans}	1.81(2)
						Cr–CO _{cis} (avg)	1.885	Cr–CO _{cis} (avg)	1.90
Bond Angles									
B–P–B'	84.3(1)	B(1)–P(1)–B(3)	113.2(3)	B(1')–P(1')–B(3')	99.7(3)	B(1)–P(1)–B(2)	81.4(4)		
		B(1)–P(2)–B(2)	103.2(3)	B(1')–P(2')–B(2')	102.3(3)	B(1)–P(2)–B(2)	82.9(4)		
		B(2)–P(3)–B(3)	101.4(3)	B(2')–P(3')–B(3')	99.4(3)				
P–B–P'	95.7(1)	P(1)–B(1)–P(2)	115.5(3)	P(1')–B(1')–P(2')	107.6(4)				
		P(2)–B(2)–P(3)	104.4(4)	P(2')–B(2')–P(3')	109.7(4)	P(1)–B(1)–P(2)	93.5(5)	P–B–P'	108.5(12)
		P(3)–B(3)–P(1)	114.7(3)	P(3')–B(3')–P(1')	114.4(3)	P(1)–B(2)–P(2)	92.6(4)		
P–B–N	129.8(2)	P(1)–B(1)–N(1)	125.5(5)	P(1')–B(1')–N(1')	128.9(5)	P(1)–B(1)–N(1)	130.7(7)	P–B–N	125.7(6)
		P(2)–B(1)–N(1)	118.4(5)	P(2')–B(1')–N(1')	123.1(5)	P(2)–B(1)–N(1)	135.7(7)		
P'–B–N	134.5(2)	P(2)–B(2)–N(3)	128.3(5)	P(2')–B(2')–N(2')	120.7(4)	P(1)–B(2)–N(2)	130.5(7)	P'–B–N	125.7(6)
		P(3)–B(2)–N(3)	126.8(5)	P(3')–B(2')–N(2')	129.4(6)	P(2)–B(2)–N(2)	136.8(7)		
		P(1)–B(3)–N(2)	125.2(5)	P(1')–B(3')–N(3')	124.0(5)				
		P(3)–B(3)–N(2)	119.8(5)	P(3')–B(3')–N(3')	121.6(5)				
B–N–C(1)	120.1(2)	B(1)–N(1)–C(1)	127.0(5)	B(1')–N(1')–C(1')	126.4(6)	B(1)–N(1)–C(6)	120.6(7)	B–N–C(6)	123.2
		B(3)–N(2)–C(13)	120.6(5)	B(2')–N(2')–C(7')	121.1(6)	B(1)–N(1)–C(9)	124.5(8)	B–N–C(6')	123.3(11)
		B(2)–N(3)–C(7)	125.4(5)	B(3')–N(3')–C(13')	128.1(6)				
B–N–C(4)	124.5(2)	B(1)–N(1)–C(4)	121.0(5)	B(1')–N(1')–C(4')	120.3(5)				
		B(3)–N(2)–C(16)	125.6(5)	B(2')–N(2')–C(10')	125.5(5)	B(2)–N(2)–C(12)	123.5(7)		
		B(2)–N(3)–C(10)	123.0(6)	B(3')–N(3')–C(16')	120.7(6)	B(2)–N(2)–C(15)	121.3(8)		
C(1)–N–C(4)	115.5(2)	C(1)–N(1)–C(4)	111.7(4)	C(1')–N(1')–C(4')	113.2(6)	C(6)N(1)–C(9)	114.9(7)	C(6)–N–C(6')	113.4(2)
		C(13)–N(2)–C(16)	113.4(5)	C(7')–N(2')–C(10')	113.4(6)	C(12)–N(2)–C(15)	115.1(7)		
		C(7)–N(3)–C(10)	111.4(6)	C(13')–N(3')–C(16')	111.3(6)				

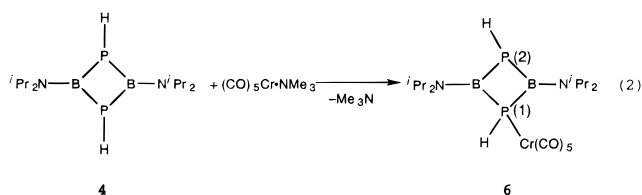
the partial overlap of two doublets in the proton coupled ³¹P NMR spectrum. The ¹¹B{¹H} NMR spectrum reveals a single resonance δ 47.1 that falls in the region expected for three-coordinate aminoborane fragments.¹⁹ The ¹³C{¹H} NMR spectrum contains a singlet at δ 23.2 assigned to equivalent ⁱPr methyl groups and a triplet at δ 51.6 (³J_{PC} = 5.0 Hz) assigned to equivalent ⁱPr methine groups. The ¹H NMR spectrum shows a doublet at δ 1.18 (³J_{HH} = 6.8 Hz) (methyl groups), a septet at δ 3.54 (³J_{HH} = 6.8 Hz) (methine groups), and a doublet centered at δ 3.43 (¹J_{PH} = 244.3 Hz) (P–H groups).

The four-membered ring structure of **4** has been confirmed by single crystal X-ray diffraction analysis, and a view of the molecule is shown in Figure 1. Selected bond lengths and angles are summarized in Table 7. The compound is centrosymmetric, and the geometry at the boron atoms is trigonal planar, while that at the phosphorus atoms is pyramidal with a *trans* disposition of the P–H bonds. Each phosphane H atom is disordered over two sites with equal occupancies. The B, P, N, B', P', and N' atoms lie in a plane, and the internal B–P–B' and P–B–P' angles are 84.3(1)° and 95.7(1)°, respectively. These values are comparable with those reported for other 1,3,2,4-diphosphadiboretanes.³ The average B–P distance, 1.931(3) Å, is intermediate in the range of B–P single bond lengths (1.896–2.041 Å).³ The *exo* B–N bond length, 1.377(3) Å, is short, and this is consistent with the presence of significant B–N π overlap.

Combination of (CO)₅Cr·NMe₃ with the diphosphadiboretane **4** ligand produced *in situ*, for example, in a 1:1.7 ratio reaction

**Figure 1.** Molecular structure and atom labeling scheme for (ⁱPr₂NBPH)₂ (**4**).

of ⁱPr₂NBCl₂ with LiPH₂·DME gives the monometallic complex **6** (eq 2). In fact, isolation of **6** in low yield (14%) from this



reaction provides confirmation of the previous NMR observation⁹ that **4** is formed in only small amounts from 1:1–1:2 reactant ratios. Compound **6** can be formed in higher yields from pure samples of **4** obtained from the protonation reaction of the lithium phosphide salt (eq 1) described herein. All efforts to obtain a bis-metal complex [(CO)₅Cr]₂·**4** were unsuccessful.

(19) Nöth, H.; Wrackmeyer, B. *Nuclear Magnetic Resonance Spectroscopy of Boron Compounds*; Springer-Verlag: West Berlin, 1978.

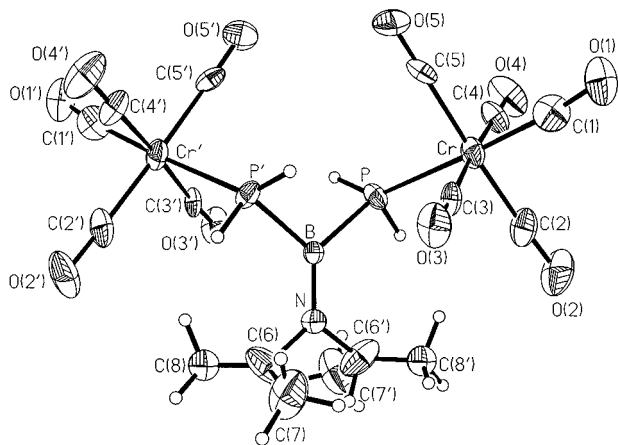


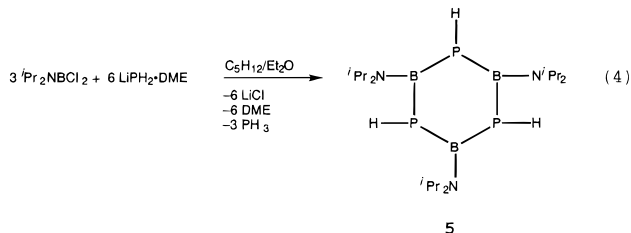
Figure 3. Molecular structure and atom labeling scheme for $i\text{Pr}_2\text{NB}[\text{PH}_2\cdot\text{Cr}(\text{CO})_5]_2$ (**7**).

parent ion in the EI mass spectrum. The infrared spectrum of **7** should show two P–H vibrations; however, only one weak band is resolved at 2349 cm^{-1} . A three-band pattern is observed in the carbonyl stretch region at 2065 , 1985 , and 1948 cm^{-1} , as expected for $\text{Cr}(\text{CO})_5\text{L}$ fragments (*vide supra*).

A single, broad resonance centered at δ 41.4 is observed in the ^{11}B NMR spectrum of **7** slightly upfield of the resonance recorded for the free ligand, δ 48.9. The $^{31}\text{P}\{^1\text{H}\}$ NMR spectrum displays a single resonance at δ -127.9 shifted significantly downfield from the free ligand δ -191.7 . Restoration of proton coupling produces a triplet with $^1J_{\text{PH}} = 310\text{ Hz}$. The $^{13}\text{C}\{^1\text{H}\}$ NMR spectrum exhibits single resonances at δ 23.0 and 53.9 that are assigned to the equivalent $i\text{Pr}$ methyl and methine carbon atoms. The $^{13}\text{C}\{^1\text{H}\}$ NMR spectrum also shows two pseudotriplet resonances in the carbonyl region at δ 216.7 and 220.8 with $^2J_{\text{PC}} = 5.4\text{ Hz}$ and $^2J_{\text{PC}} = 3.2\text{ Hz}$, respectively. The ^1H NMR spectrum reveals equivalent phosphane δ 3.0, methyl δ 0.85 (doublet $^3J_{\text{HH}} = 6.8\text{ Hz}$), and methine, δ 3.1 (septet $^3J_{\text{HH}} = 6.8\text{ Hz}$), environments. Taken together, these data are consistent with a highly symmetric structure.

The single crystal X-ray diffraction analysis of **7** confirms the bimetallic structure and, by inference, confirms the existence of ligand **8**. A view of the complex is shown in Figure 3. The molecule sits on a crystallographic 2-fold axis that passes through the B and N atoms. The N, B, and two P atoms form a plane, and the two phosphorus atoms are tetrahedral. The P–B bond length, $1.95(1)\text{ \AA}$, falls in the single bond range, and the B–N bond length, $1.37(3)\text{ \AA}$, is short. The $\text{Cr}(\text{CO})_5\text{P}$ units are pseudooctahedral with a Cr–P distance of $2.385(5)\text{ \AA}$ and a *trans* Cr–C(O) distance of $1.81(2)\text{ \AA}$. These data, as in **6**, indicate that ligand **8** acts as a modest σ donor and a poor π acceptor ligand.

With this information available, the only remaining unconfirmed or unidentified species in the $i\text{Pr}_2\text{NBCl}_2/\text{LiPH}_2\cdot\text{DME}$ system described previously⁹ is that responsible for the relatively broad resonance centered at δ -151 in the $^{31}\text{P}\{^1\text{H}\}$ NMR spectrum. In the current study, it is found that the yield of this compound **5** is maximized when the 1:2 reaction of $i\text{Pr}_2\text{NBCl}_2$ and $\text{LiPH}_2\cdot\text{DME}$ in Et_2O /pentane solution (eq 4) is performed under an inert atmosphere in a Schlenk vessel left open to a mercury bubbler. The PH_3 evolved in the reaction is allowed to escape through the bubbler, or it can be swept from the vessel with a very slow stream of nitrogen. If the PH_3 is not allowed to escape, then complex reaction mixtures are obtained that contain relatively small amounts of **5**. Compound **5** is obtained as a faintly yellow oil that slowly crystallizes as colorless, well-



formed prisms that are soluble in Et_2O , benzene, toluene, pentane, and hexane.

Compound **5** displays a weak parent ion in the high-resolution-FABS mass spectrum with the observed mass 429.3095 in good agreement with the calculated value for $\text{C}_{18}\text{H}_{42}\text{N}_3^{11}\text{B}_3^{31}\text{P}_3$, 429.31111 (deviation = 1.27 ppm), corresponding to the six-membered ring compound $(i\text{Pr}_2\text{NBPH})_3$. The compound displays a single P–H stretching band at 2313 cm^{-1} in the infrared spectrum. The $^{11}\text{B}\{^1\text{H}\}$ NMR spectrum shows a single resonance centered at δ 49.8. The room temperature $^{31}\text{P}\{^1\text{H}\}$ NMR spectrum of **5** in C_6D_6 or C_7D_8 displays a single, broad ($W_{1/2} \sim 250\text{ Hz}$) resonance centered at δ -151 , as found in spectra for samples that contain the previously unidentified species. This spectrum is strongly temperature dependent (Figure 4). Cooling the sample to $10\text{ }^\circ\text{C}$ results in additional line broadening ($W_{1/2} \sim 600\text{ Hz}$), and at $0\text{ }^\circ\text{C}$, an upfield shoulder appears on the primary resonance. At $-10\text{ }^\circ\text{C}$, this shoulder is resolved into a separate peak (δ -163), and at $-20\text{ }^\circ\text{C}$, a third resonance (δ -145), downfield of the primary band, is seen. With continued cooling, all three peaks sharpen, and at $-40\text{ }^\circ\text{C}$, a fourth sharp resonance begins to separate from the peak at δ -151 . At $-60\text{ }^\circ\text{C}$, this resonance is fully resolved at δ -152.9 . With application of an exponential line broadening factor ($\text{LB} = 0.1\text{ Hz}$), the spectrum at $-60\text{ }^\circ\text{C}$ shows three resonances of similar intensity centered at δ -143.8 , -152.9 , and -164.2 . The middle of these two bands displays some evidence of a doublet structure, $J \sim 67\text{ Hz}$. This pattern is consistent with an ABC second-order spin system that might be expected for an asymmetric nonplanar B_3P_3 six-membered ring. In addition, the spectrum contains a strong, sharp resonance at δ -151.3 .

The observed $^{31}\text{P}\{^1\text{H}\}$ NMR data suggested that further treatment of the FID might reveal additional coupling data. Indeed, line narrowing accomplished by application of a Gauss function revealed further splitting of the resonances centered at δ -143.8 , -152.9 , and -164.2 . The resonance at δ -151.3 was unaffected. The final spectrum, along with a simulation, is shown in Figure 5. The simulation provides coupling constants, $J_{\text{AB}} = 28\text{ Hz}$, $J_{\text{AC}} = 49\text{ Hz}$, $J_{\text{BC}} = 123\text{ Hz}$, and from the proton-coupled spectrum at $-60\text{ }^\circ\text{C}$ are extracted $^1J_{\text{PH}} = 228$, 218 , and 180 Hz . The ^1H and $^{13}\text{C}\{^1\text{H}\}$ NMR spectra are also temperature dependent. At $20\text{ }^\circ\text{C}$, the $^{13}\text{C}\{^1\text{H}\}$ spectrum displays single CH (δ 51.2 $W_{1/2} = 120\text{ Hz}$) and CH_3 (δ 22.8) environments, while at $-50\text{ }^\circ\text{C}$, two CH (δ 55.1, 46.8) and two CH_3 (δ 24.1, 20.8) resonances are found. The ^1H NMR spectrum at $-50\text{ }^\circ\text{C}$ also displays two CH_3 resonances, but only one CH resonance is resolved.

The collective NMR data suggest that, at $20\text{ }^\circ\text{C}$, the six-membered ring is involved in dynamic motional processes. Cooling solutions of **5** apparently slows the equilibration, and in the temperature range -50 to $-60\text{ }^\circ\text{C}$, resonances for two geometrical isomers appear. One is highly symmetrical, giving rise to a single sharp resonance in the $^{31}\text{P}\{^1\text{H}\}$ spectrum at δ -151.3 . This is likely a chair isomer. The second, less symmetrical molecule gives rise to the ABC second-order pattern and may correspond to a twisted chair or twisted boat isomer.

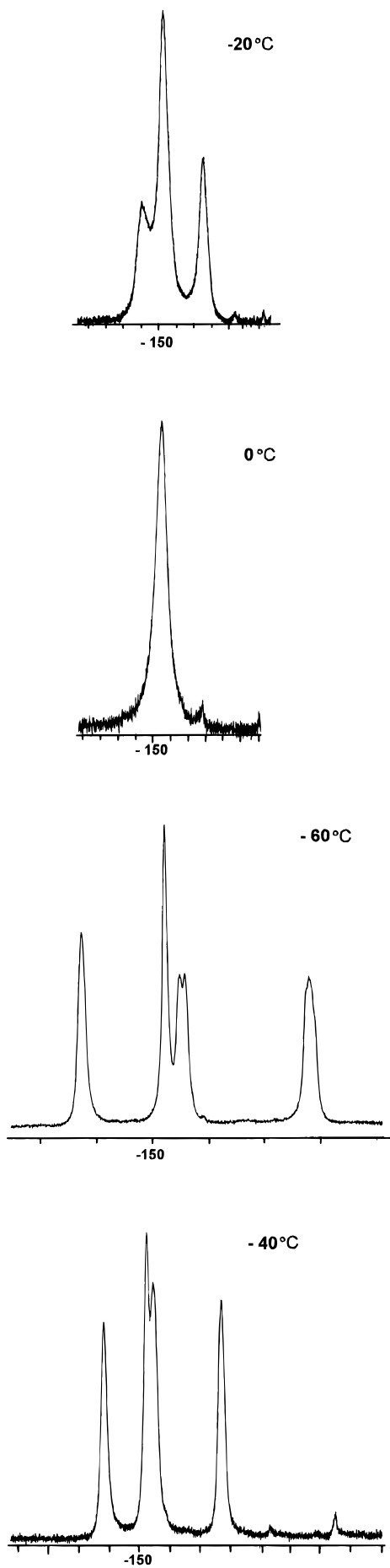


Figure 4. Variable temperature $^{31}\text{P} \{^1\text{H}\}$ NMR spectrum for $(i\text{Pr}_2\text{NBPH})_3$ (5).

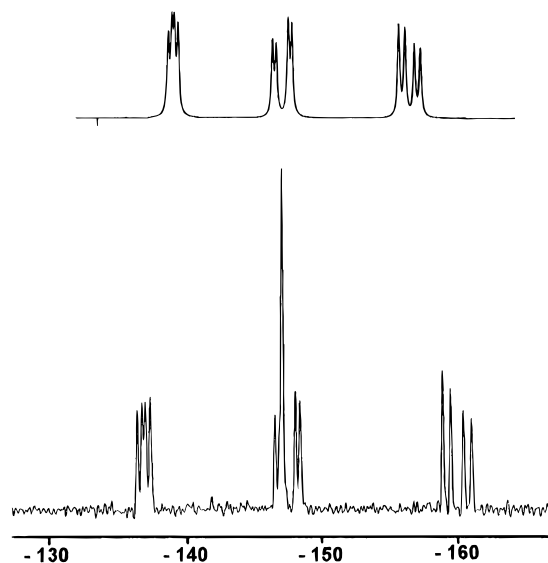


Figure 5. Observed and simulated $^{31}\text{P} \{^1\text{H}\}$ NMR spectrum for $(i\text{Pr}_2\text{NBPH})_3$ (5), at -60°C .

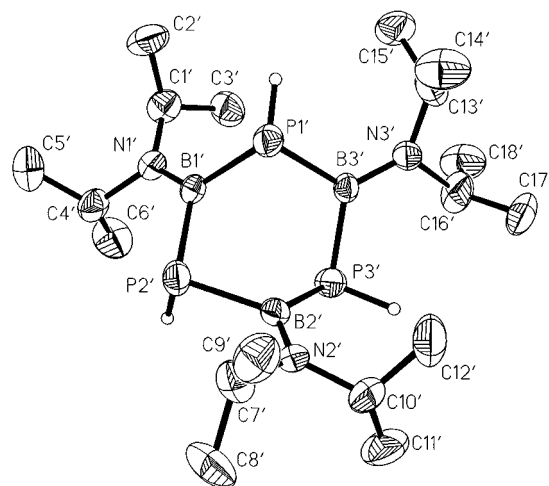


Figure 6. Molecular structure and atom labeling scheme for $(i\text{Pr}_2\text{NBPH})_3$ (5) (molecule 1).

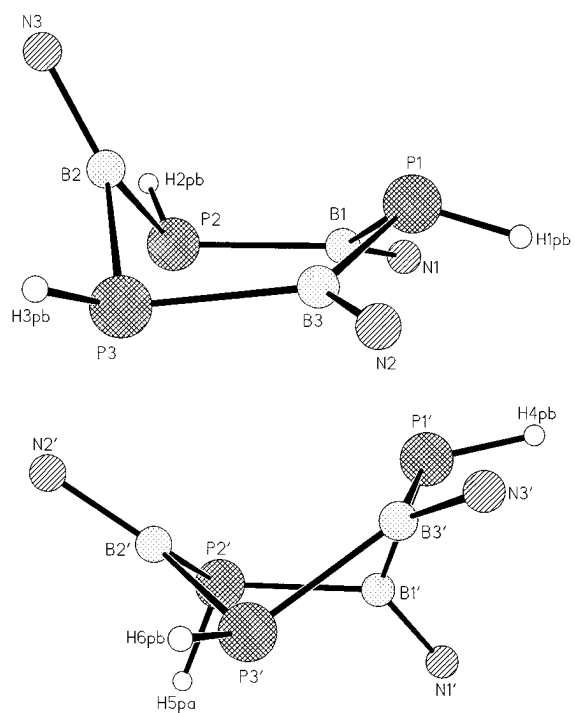


Figure 7. Ring conformations for 5 molecules 1 and 2.

The solid-state molecular structure of **5** has been determined by single crystal X-ray diffraction techniques. There are two independent molecules per asymmetric unit, and an ORTEP view of molecule 1 is shown in Figure 6, and bond lengths and angles are summarized in Table 7. Framework presentations of both molecules presented in Figure 7 reveal twisted, boat-like, six-membered ring conformations. The boron atoms have a trigonal planar geometry, and the phosphorus atoms have a pyramidal geometry with the P–H vectors in equatorial positions. The average B–P bond length, 1.933 Å (range 1.911–1.947 Å), is clearly in the single bond range, and it contrasts markedly with the distances in the planar pseudoaromatic species (MesBPCy)₃ 1.839 Å⁷ and (MesBPh)₃ 1.842 Å.⁸ The average B–P bond length in **5** is comparable to the average value for the twisted cyclohexane-like analog [(Me₃Si)₂NBPH]₃, 1.928 Å. As would be expected, the *exo* B–N bonds in **5** are short (average 1.393 Å), indicative of significant B=N π overlap.

With a reliable high-yield synthesis for **5** in hand, it should be possible to study its coordination chemistry with metal carbonyl fragments. Unfortunately, reactions of **5** with various

amounts of (CO)₅Mo·NMe₃ at this point have given only inseparable mixtures of products. Further efforts will be required to elucidate the coordination behavior as well as the utility of the ring as an assembly platform for the construction of new boron–phosphorus cage compounds.

Acknowledgment is made to the National Science Foundation (Grant CHE-9508668) (R.T.P.) and the Fonds der Chemischen Industrie (H.N.) for support of this work. Support from the Department of Energy URIP (Grant De-FG05-75294) assisted purchase of the JEOL GSX-400 NMR spectrometer. Selected mass spectral determinations were made at the Midwest Center for Mass Spectrometry with partial support of the NSF Biology Division (Grant DIR-9017262).

Supporting Information Available: Tables containing details of the X-ray data collection and refinement, hydrogen atom coordinates, thermal parameters, and complete bond distances and angles (29 pages). Ordering information is given on any current masthead page.

IC9514399